Journal of Building Engineering 96 (2024) 110447

Contents lists available at ScienceDirect

Journal of Building Engineering

journal homepage: www.elsevier.com/locate/jobe

Implications of latent and sensible building energy loads using natural ventilation

Mojtaba Safdari [a], Kadeem Dennis [b], Bahram Gharabaghi [a], Kamran Siddiqui [b], Amir A. Aliabadi [a,*]

[a] School of Engineering, University of Guelph, Guelph, Ontario, Canada
[b] Department of Mechanical and Materials Engineering, Western University, London, Ontario, Canada

ARTICLE INFO

Dataset link: http://www.aaa-scientists.com/, https://github.com/AmirAAliabadi

Keywords:
Advanced controllers
Energy consumption
HVAC
Natural ventilation
Smart buildings

ABSTRACT

Building decarbonization requires balancing energy efficiency with occupant comfort. Sensible cooling and latent loads, traditionally addressed by air conditioning, are significant contributors to energy use. This study explores an innovative approach to utilize natural ventilation through windows when outdoor conditions are favorable. The novelty of this work lies in its comprehensive consideration of sensible and latent loads, including both humidification and dehumidification, within the context of natural ventilation. When in cooling mode, if the indoor temperature rises above the cooling set point and the outdoor temperature is lower than the indoor temperature, the windows will automatically open to enhance natural ventilation, provided the specific humidity conditions for indoor, outdoor, and set point are met. Simulations using the Vertical City Weather Generator (VCWG v1.4.7) software investigate the energy savings potential in Toronto, Vancouver, and Phoenix for 2020. Results indicate potential for notable annual total cooling load savings of 5–15 kW-hr m^{-2} $Year^{-1}$. Additionally, further analyses examine the impact of building air-tightness, envelope thermal resistance, and climate zone on the effectiveness of natural ventilation to reduce the sensible cooling, latent, and total cooling loads.

1. Introduction

The escalating energy demand for building Heating, Ventilation, and Air-Conditioning (HVAC) systems is a global concern, with buildings accounting for over 30% of global final energy consumption and 26% of global energy-related emissions according to a 2021 report by the International Energy Agency (IEA). As a result, there is a growing focus on assessing the impact of ventilation strategies on building energy needs, with Natural Ventilation (NV) emerging as a promising approach [1]. Studies have shown that buildings with well-designed NV systems can achieve significant reductions in cooling energy and air conditioning costs [2,3].

There are various ventilation methods employed in buildings, each with its own advantages and limitations. Mechanical Ventilation (MV) [4–6] utilizes fans and air conditioning systems to actively control indoor air temperature and humidity. While MV systems offer precise control and can function independently of outdoor conditions, they rely on continuous energy consumption. Modern structures, including living units, workspaces, and large buildings, rely on MV systems for controlled Indoor Air Quality (IAQ) and occupant comfort [7].

* Corresponding author.
E-mail addresses: msafdari@uoguelph.ca (M. Safdari), aaliabad@uoguelph.ca (A.A. Aliabadi).
URL: https://www.aaa-scientists.com (A.A. Aliabadi).

https://doi.org/10.1016/j.jobe.2024.110447
Received 11 June 2024; Received in revised form 22 July 2024; Accepted 11 August 2024
Available online 20 August 2024

In living units, MV systems reduce the presence of air contaminants (e.g., carbon dioxide, Volatile Organic Compounds (VOCs), and atmospheric particulates), improving occupants' health. Additionally, they maintain optimal moisture levels, preventing mold growth [8]. Recent advancements have integrated MV systems with advanced sensor networks, intelligent algorithms, and Internet of Things (IoT) technologies, leading to optimized ventilation settings and improved IAQ while reducing energy consumption. IoT-enabled smart MV systems in living units have demonstrated significant improvements in both air quality and energy efficiency by facilitating real-time monitoring and control, enhancing system's responsiveness and adaptability [9–12].

Similarly, MV systems in work spaces enhance workers' comfort and hence productivity by managing indoor pollutants, temperature, and moisture levels [13–15]. Poor IAQ or thermal comfort can negatively impact attendance and performance [16]. Advanced MV systems incorporate sensors and automation to adjust airflow based on occupancy and air quality metrics, optimizing energy use while maintaining high IAQ and thermal comfort standards [17]. The integration of advanced algorithms further improves efficiency and effectiveness [18].

For large buildings like schools, sport facilities, and hospitals, MV systems are essential for consistent IAQ and thermal comfort [19–21]. While passive design strategies reduce energy consumption, supplemental MV is often necessary [22]. These buildings utilize sophisticated control methods, adjusting ventilation parameters based on real-time data [23,24]. This ensures efficient ventilation, enhanced energy performance, and a healthy indoor environment.

In contrast to MV, NV systems offer a passive approach that uses natural forces like wind [25] and buoyancy-driven [26] pressure differences to exchange air with the surrounding environment. This not only reduces energy consumption [27] but also provides a more sustainable solution for building cooling. The effectiveness of NV systems depends heavily on factors such as outdoor temperature and humidity [28], wind patterns, building design [29], and the careful placement and operation of windows, doors, and vents [30]. Recent advancements in Artificial Intelligence (AI)-powered building management systems allow for the optimization of NV strategies by analyzing real-time weather data, occupant needs, and building characteristics, leading to further energy savings and improved occupant comfort [31].

Buildings with sophisticated NV systems can significantly reduce their air conditioning costs. There are different ways buildings can be ventilated based on the method used for air exchange [32,33]. Air mass can be displaced due to several methods such as wind, buoyancy, humidity difference, and mechanical equipment. NV systems offer a passive approach where the building uses wind and/or buoyancy to exchange air with the surroundings to control indoor temperature and provide fresh air. This relies on how the vents and windows are designed, placed, and operated in the building [30]. NV systems require minimal capital investment, very low energy input, and low maintenance costs. NV systems are reliable and eco-friendly, especially during power outages and emergencies, which give another option when MV systems are not functional. However, NV systems need the right outdoor/indoor temperature and humidity conditions. Beyond purely MV or NV systems, a hybrid ventilation system can combine both MV and NV systems to capitalize on their strengths [34].

Several studies have explored the application of NV systems in buildings, investigating various systems like Trombe walls [35], wind towers [36], and wind catchers [37]. For instance, [38] investigated how air channel width and ventilation strategy (natural versus mechanical) impact Trombe wall heat transfer. They built an adjustable channel to test these factors and found that mechanical ventilation improves performance, particularly in cloudy weather situations. Finally, they parameterized models to predict heat transfer based on these factors [38].

Recent advances in NV have significantly enhanced its efficiency and applicability in modern building design. Innovations, such as smart ventilation systems, now integrate Internet of Things (IoT) sensors and AI algorithms to dynamically adjust ventilation strategies based on real-time environmental data and occupancy patterns [39]. For example, adaptive control systems can automatically modulate window openings and vent positions to optimize air flow and indoor air quality while minimizing energy usage [40]. [41] used Reinforcement Learning (RL) to optimize HVAC systems that utilize natural ventilation. Their RL method, based on Q-learning, controls both HVAC and windows to minimize energy use and occupant discomfort. Simulations showed significant improvements over traditional rules-based controls, especially in reducing energy consumption and discomfort. These systems can also predict and respond to changes in weather conditions, such as sudden rain or temperature shifts, ensuring consistent indoor comfort. Additionally, advancements in Building Information Modeling (BIM) allow for the seamless integration of NV systems in the design phase, enabling architects and engineers to simulate and optimize ventilation performance before construction [42]. Further, the use of renewable energy sources to power these smart systems enhances their sustainability [43].

Another study proposed a fuzzy control strategy as an approach for managing naturally ventilated buildings [44]. This method exploits linguistic rules to adjust window openings based on external wind velocity, direction, and temperature. The objective was to achieve thermal comfort and adequate air distribution within the building. The study investigated two fuzzy control models with varying numbers of membership functions and IF-THEN rules. The results demonstrated that the model with a higher number of membership functions performed better, responding more effectively to changing outdoor conditions and maintaining comfortable indoor temperatures.

Limited research has been conducted to investigate the latent load implications of NV and humidity control over long-term up to a full year [43]. It is true that NV helps reducing the sensible cooling load of buildings, but opening doors and windows may make indoor spaces too humid or dry, resulting in added latent loads. The confounding role of humidity control is studied in the context of NV systems to a lesser extent. In fact, most studies lack real-world data on hourly outdoor air temperature and humidity fluctuations, which significantly impact the NV systems' efficacy. Finally, there is need to assess the potential of NV schemes in building energy savings for different Climate Zones (CZ).

This study addresses these gaps by analyzing the potential of NV systems for residential buildings in Toronto (CZ5), Vancouver (CZ4), and Phoenix (CZ3) using an urban physics model titled the Vertical City Weather Generator (VCWG v1.4.7). A rules-based

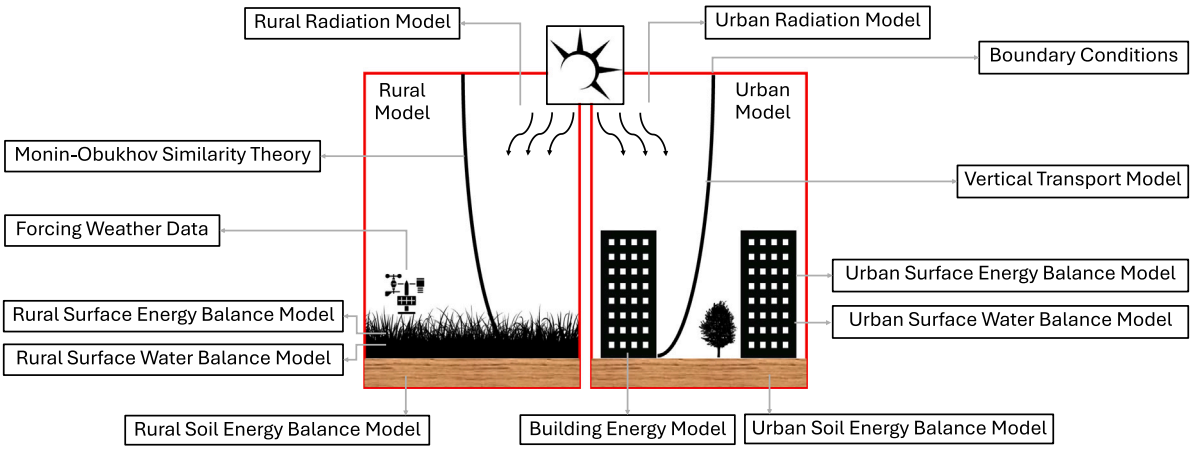

Fig. 1. Overview of the Vertical City Weather Generator (VCWG v1.4.7) model and the integration of sub-models.

controller is implemented to operate windows when indoor/outdoor temperature and specific humidities are favorable. We will investigate the sensible cooling load, latent load, and hence the total cooling load as a result of implementing NV. The novelty of this work is the consideration of humidity and latent load, including humidification and dehumidification, in NV, which has not been properly studied before. We analyze the cooling loads for single detached residential buildings in each of the three cities for an entire year in 2020. Further, for Toronto and Vancouver, a sensitivity study is conducted to find the effectiveness of NV systems in reducing the cooling load by varying building envelope thermal resistance and infiltration rates.

The paper is organized as follows. In Section 2 we provide the methodology by introducing the VCWG model, the NV scheme, model sensitivity framework, and model validation. In Section 3 we provide the results and discussion by focusing on the sensitivity analysis and the influence of warmer climate zones for NV systems' potential. Finally, in Section 4 we offer our conclusions and recommendations for future work.

2. Methodology

2.1. Model description

Urban physics is simulated in this study by employing the Vertical City Weather Generator (VCWG v1.4.7) software (Fig. 1). VCWG is a multi-physics and micro-scale model to parameterize numerous physical processes and integrate them to make predictions on urban climate and building performance variables. VCWG integrates models at the system level with various physical processes for exchanges of momentum, heat, humidity, and water through soil, urban surfaces, and the atmosphere as well as options for integrating alternative energy systems. VCWG integrates models using the Resistance Capacitance (RC) thermal network, Navier–Stokes transport modeling in the vertical direction, Monin–Obukhov Similarity Theory (MOST), and bulk energy modeling paradigms [45]. As shown in Fig. 1, VCWG is comprised of various sub-models: a rural MOST model, an urban vertical transport model, rural/urban radiation models, a building energy model, rural/urban soil energy balance models, and rural/urban surface energy/water balance models. Full descriptions of the model are provided in earlier publications [46–50]. The weather boundary conditions for VCWG are generated using another software titled the Vatic Weather File Generator (VWFG v1.0.0), which uses the ERA5 dataset from the European Centre for Medium-Range Weather Forecasts (ECMWF). VWFG provides data in the EnergyPlus Weather (EPW) file format at hourly resolution that is required by VCWG. The forcing weather files are associated with a rural site in the vicinity of each city [51].

Fig. 2 shows the arrangement of single detached residential buildings considered in this study. Such houses are prevalent in North America and account for 52.6% and 64% of residential building stock in Canada [52] and the United States [53], respectively. The building features for each city are based on common codes and standards such as the National Energy Code of Canada for Buildings (NECB) [54], the American Society of Heating, Refrigerating and Air-Conditioning Engineers (ASHRAE) 62.1 [55], ASHRAE 62.2 [56], ASHRAE 90.1 [57], and ASHRAE 90.2 [58]. Table 1 shows the code and standard values for the base building features.

The buildings are arranged in rows with a separation of 30 m maintained in each horizontal direction (x and y). Temperature, specific humidity, and wind (the x and y components) data within the urban roughness sub-layer were extracted along the vertical direction (z) from VCWG. The buildings are low-rise residential units designed with dimensions of 13.8 m × 13.8 m × 6 m. Each story features two windows on each side, with an equivalent area of 26.4 m^2 per facade. The NV system model assumes a single equivalent window on each building side and is based on the ASHRAE Handbook - Fundamentals [59]. The calculation of the NV system air flow rate is performed by the following formula:

$$Q = CAU, \tag{1}$$

Table 1
Building features for Climate Zones (CZ) 3, 4, and 5 from codes and standards.

Parameter	Phoenix (CZ3)	Vancouver (CZ4)	Toronto (CZ5)
Roof Resistance [m^2 K W^{-1}]	4.40	5.18	6.41
Wall Resistance [m^2 K W^{-1}]	2.30	3.17	3.6
Window U-value [W m^{-2} K^{-1}]	2.84	2.1	1.9
Infiltration Rate [ACH]	3.0	3.0	3.0
Ventilation Rate [L s^{-1} m^{-2}]	0.3	0.3	0.3
Glazing Ratio [–]	0.4	0.4	0.4
Solar Heat Gain Coefficient [–]	0.25	0.4	0.4

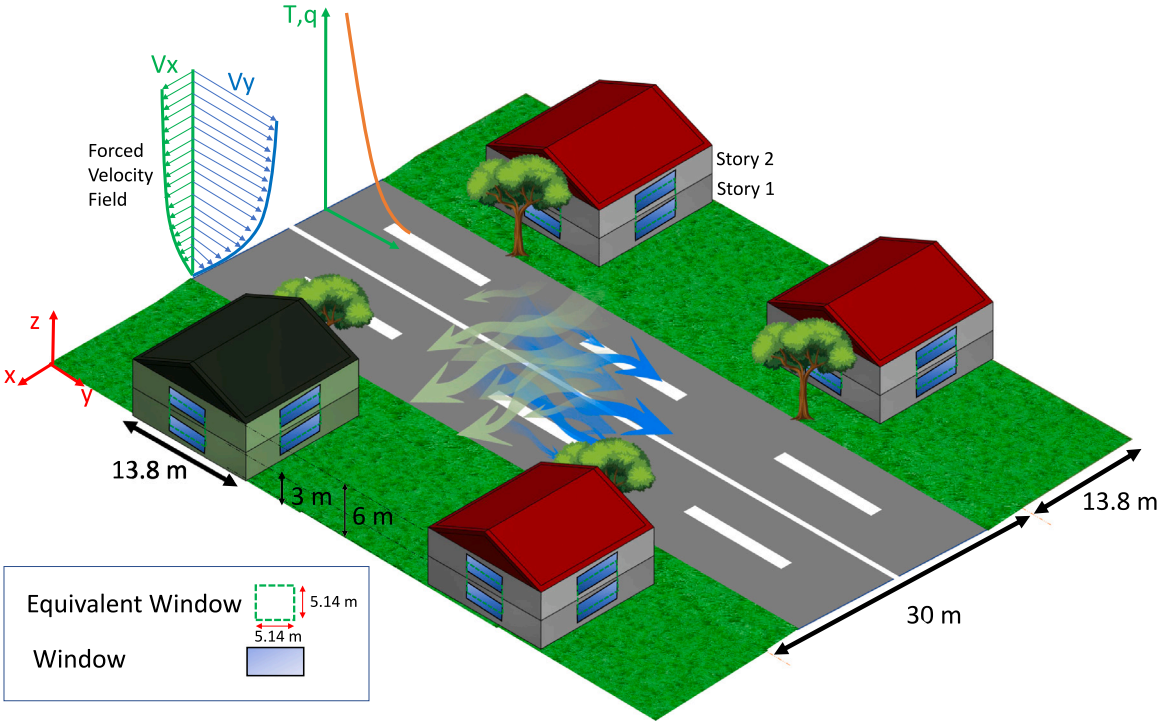

Fig. 2. Visualization of buildings' arrangements and outdoor weather variables simulated by the Vertical City Weather Generator (v1.4.7); T: temperature, q: specific humidity, V_x and V_y: horizontal components of wind velocity vector.

where Q [m^3 s^{-1}] is flow rate, $C = 0.5$ [-] is a coefficient describing the effectiveness of windows (based on [59], it can be assumed to be 0.5 to 0.6 for normal winds and 0.25 to 0.35 for diagonal winds), A [m^2] is the free area of inlet openings, and U [m s^{-1}] is the wind speed normal to the facade.

The sensible and latent energy balances of the building under cooling mode are illustrated in Figs. 3 and 4, showing the sensible and latent loads on the building, respectively. Fig. 3 shows the components of the sensible cooling load, set-point, indoor, and outdoor temperatures for an instance when the window would be opened for NV. The sensible load,

$$Q_{\text{vent}} + Q_{\text{inf}} + Q_{\text{NV}} = \underbrace{Q_{\text{int}} + Q_{\text{mass}} + Q_{\text{wall}} + Q_{\text{ceil}} + Q_{\text{win}} + Q_{\text{tran}}}_{\text{Sensible Cooling Load}}, \tag{2}$$

involves internal heat from occupants and equipment Q_{int}, heat from the building's mass Q_{mass}, heat from walls Q_{wall}, heat from ceilings Q_{ceil}, heat conduction through windows Q_{win}, and radiant heat passing through windows Q_{tran} [W]. Except for Q_{int}, which is scheduled in VCWG, the other terms are parameterized using the heat balance method:

$$\begin{aligned}
Q_{\text{mass}} &= A_{\text{bui}} h_m (T_{\text{mass}} - T_{\text{set}}) \\
Q_{\text{wall}} &= A_{\text{wall}} h_w (T_{\text{wall}} - T_{\text{set}}) \\
Q_{\text{ceil}} &= A_{\text{bui}} h_c (T_{\text{ceil}} - T_{\text{set}}) \\
Q_{\text{win}} &= A_{\text{win}} U_w (T_{\text{outdoor}} - T_{\text{set}}) \\
Q_{\text{tran}} &= A_{\text{win}} S \times SHGC,
\end{aligned} \tag{3}$$

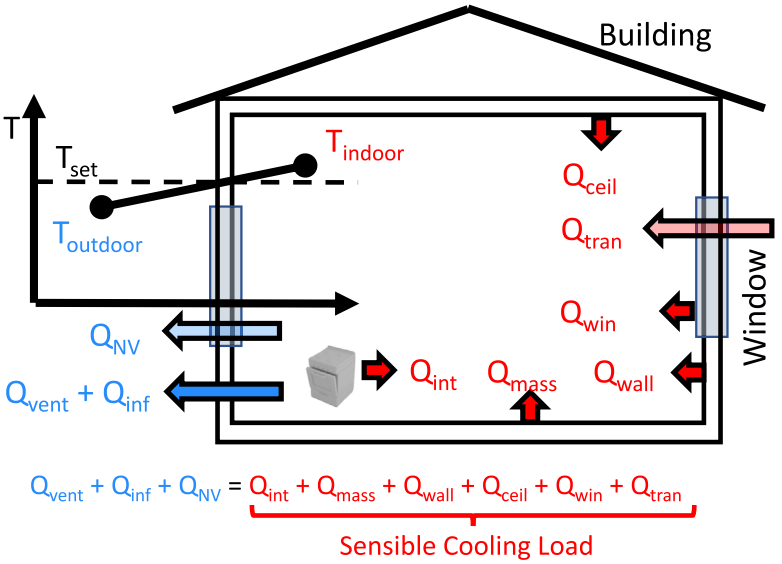

Fig. 3. Sensible energy balance for a building under cooling condition with assistance of natural ventilation.

where A_{bui} [m^2] is building footprint area, T_{mass}, T_{wall}, T_{ceil}, T_{set}, and $T_{outdoor}$ [°C] are mass, wall, ceiling, set-point, and outdoor temperatures, A_{bui}, A_{wall}, and A_{win} [m^2] are building footprint, wall, and window areas, h_m, h_w, and h_c [W m^{-2} °C^{-1}] are convective heat transfer coefficients, U_w [W m^{-2} °C^{-1}] is the window U-value, S [W m^{-2}] is the shortwave radiation flux through the window, and $SHGC$ [-] is the solar heat gain coefficient for the window. These loads are met by the building's cooling equipment Q_{vent}, infiltration Q_{inf}, and NV through windows Q_{NV} [W]. In VCWG, Q_{inf} and Q_{NV} are parameterized as

$$\begin{aligned} Q_{\text{inf}} &= V_{\text{inf}}\rho_a c_{pa}(T_{\text{outdoor}} - T_{\text{set}}) \\ Q_{\text{NV}} &= V_{\text{NV}}\rho_a c_{pa}(T_{\text{outdoor}} - T_{\text{set}}), \end{aligned} \tag{4}$$

where V_{vent}, V_{inf}, and V_{NV} [m^3 s^{-1}] are ventilation, infiltration, and NV air flow rates, ρ_a [kg m^{-3}] is density of air, and c_{pa} [J kg^{-1} °C^{-1}] is heat capacity of air. This study aims to reduce the ventilation load Q_{vent} [W] by using natural ventilation for cooling Q_{NV} [W] through windows.

Fig. 4 shows the components of the latent load, set-point, indoor, and outdoor specific humidities for an instance when the window would be opened for NV. The latent load,

$$Q_{\text{latent}} + Q_{\text{latNV}} = \underbrace{Q_{\text{latvent}} + Q_{\text{latinf}} + Q_{\text{latint}}}_{\text{Latent Load}}, \tag{5}$$

involves latent heat from internal heat from occupants and equipment Q_{latint}, latent heat from ventilation $Q_{latvent}$, and latent heat from infiltration Q_{latint}. These loads are met by the building's humidification/dehumidification equipment Q_{latent} and latent load reduction through NV Q_{latNV} [W]. Except for Q_{latint}, which is scheduled in VCWG as a fraction of sensible heat from occupants and equipment Q_{int}, the other terms are parameterized using the humidity balance method

$$\begin{aligned} Q_{\text{latvent}} &= V_{\text{vent}}\rho_a L_v(q_{\text{outdoor}} - q_{\text{set}}) \\ Q_{\text{latinf}} &= V_{\text{inf}}\rho_a L_v(q_{\text{outdoor}} - q_{\text{set}}) \\ Q_{\text{latNV}} &= V_{\text{NV}}\rho_a L_v(q_{\text{outdoor}} - q_{\text{set}}), \end{aligned} \tag{6}$$

where L_v [J kg_v^{-1}] is latent heat of vaporization for water, and $q_{outdoor}$ and q_{set} [kg_v kg^{-1}] are outdoor and set-point specific humidities, respectively. This study aims to reduce the latent load $Q_{latvent}$.

Fig. 5 shows the rules-based algorithm for the decision to trigger NV. The algorithm begins by calculating the building's cooling load. If a positive cooling load is identified (indicating a need for cooling), the algorithm then evaluates whether window opening is suitable based on both outdoor and indoor conditions. Both temperature and specific humidity checks must be passed to trigger NV. A temperature check is performed first ($T_{set} < T_{indoor}$). If the indoor temperature exceeds the set-point temperature, the algorithm checks the outdoor temperature to be less than the indoor temperature ($T_{outdoor} < T_{indoor}$). When the outdoor temperature is lower than the indoor temperature, indicating the potential for cooling through window ventilation, the windows may be opened subject to specific humidity conditions. Following the temperature check, the algorithm transitions to assess the indoor specific humidity level. The indoor relative humidity set-points are 60% under cooling mode and 40% under heating mode for CZ4 and CZ5 (humid summers and dry winters for Toronto and Vancouver), while they are 40% under cooling mode and 60% under heating mode

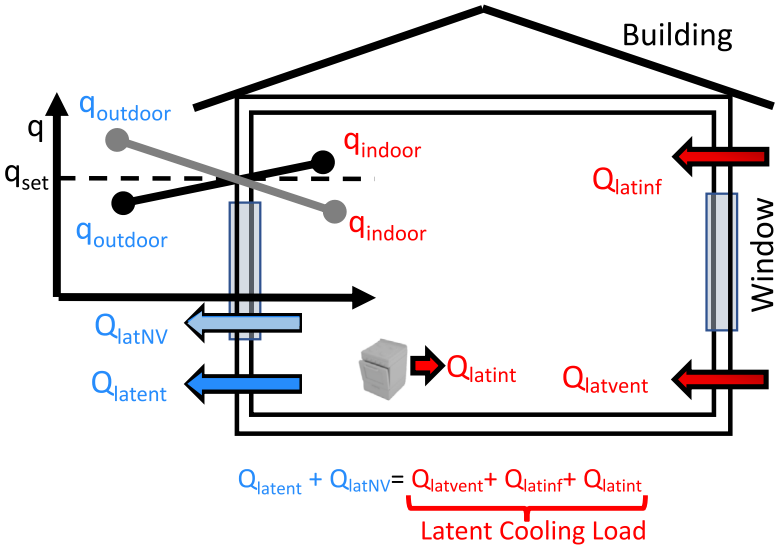

Fig. 4. Latent energy balance (humidification/dehumidification) for a building under cooling condition with assistance of natural ventilation.

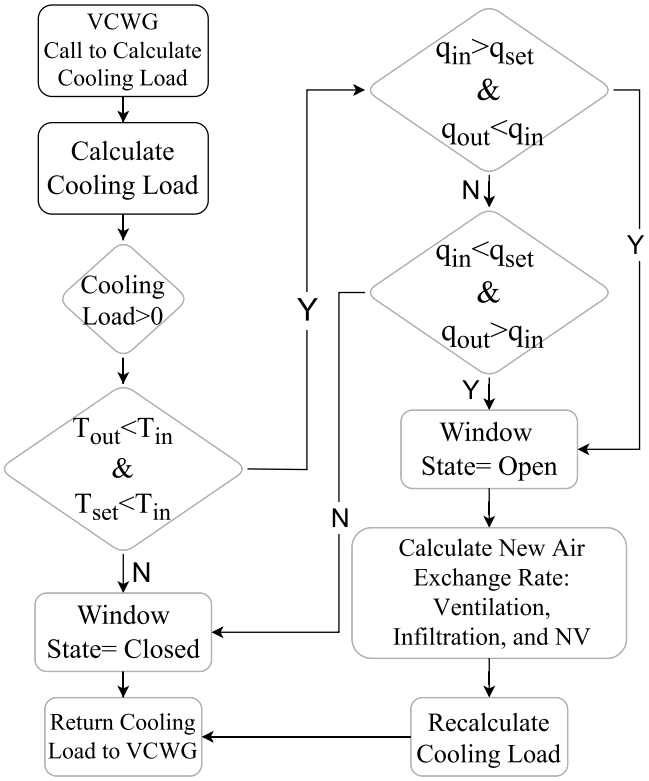

Fig. 5. Natural ventilation rules-based algorithm flowchart.

for CZ3 (dry summers and humid winters for Phoenix). After converting the relative humidity set-points to specific humidities, if $q_{indoor} > q_{set}$ & $q_{outdoor} < q_{indoor}$ (need for dehumidification) or if $q_{indoor} < q_{set}$ & $q_{outdoor} > q_{indoor}$ (need for humidification), then NV is triggered by opening the window. Finally, the newly determined air exchange rates (ventilation, infiltration, and NV) are incorporated into the sensible cooling and latent load recalculation. The recalculated values are then returned to the VCWG model.

Table 2
Design simulation points for sensitivity analysis considering infiltration rate [ACH], R-Value Increase [%], and city, as independent variables.

Input	Variable 1	Variable 2	Variable 3
Run #	A: Infiltration [ACH]	B: R-Value Increase [%]	C: City [–]
1	0.3	0.0	Vancouver
2	0.3	66.7	Vancouver
19	0.3	6.7	Vancouver
13	1.2	20.0	Vancouver
6	1.2	100.0	Vancouver
7	1.7	14.0	Vancouver
16	1.7	10.0	Vancouver
12	2.6	50.0	Vancouver
4	3.0	0.0	Vancouver
8	3.0	100.0	Vancouver
20	3.0	6.7	Vancouver
3	0.3	0.0	Toronto
10	0.3	100.0	Toronto
14	0.3	20.0	Toronto
18	1.2	6.7	Toronto
5	1.7	50.0	Toronto
17	1.7	10.0	Toronto
21	1.7	0.0	Toronto
9	3.0	100.0	Toronto
11	3.0	0.0	Toronto
15	3.0	20.0	Toronto

2.2. Sensitivity study

To assess the sensitivity of the NV system to various building features, we performed a series of numerical experiments for the case of Toronto and Vancouver. The infiltration rate in Air Changes per Hour (ACH) was varied within a range from 0.3, reflecting a Passive House standard [60], to 3, associated with a typical house. Also the base building envelope thermal resistance values were increased from zero to 100%, representative of a Passive House standard [60]. These building features are believed to strongly influence the performance of the NV system, so they were given special attention in the sensitivity analysis [50]. Utilizing these independent variables and their corresponding ranges, we generated 21 design simulation points using Design Expert (v13) software shown in Table 2. The range for infiltration received 5 additional intermediate points, while the range for R-value increase received 6 additional intermediate points. These points were strategically chosen by the software to comprehensively capture the entire spectrum of variations within the domain of variables. A combination of these points created our 21 VCWG runs.

2.3. Model validation

To validate the accuracy of VCWG in predicting the HVAC energy consumption, its predictions of electricity and gas consumption were compared against actual energy consumption for London, Ontario (CZ5) for a full year. We compared the model predictions to real observations of total monthly electricity and annual gas consumption in a neighborhood with 29 premises in 2019.

For gas consumption, the neighborhood data showed a value of 25.22 m^3_{gas} m^{-2} $Year^{-1}$, while the VCWG model predicted a value of 24.97 m^3_{gas} m^{-2} $Year^{-1}$, demonstrating an agreement within ±0.9%. For electricity consumption, Fig. 6 shows the monthly electricity consumption as predicted by VCWG and observed for London. The comparison achieves an agreement within ±6.0%. Furthermore, the plot clearly reveals the seasonal trend in electricity usage, with peaks during warm months and sharp decreases towards colder months, which the model predicts reasonably well. ASHRAE Standard 140 [61] and ASHRAE Guideline 14 [62] establish a framework for comparing building energy models against observations, and they deem a model acceptable if it predicts energy consumption successfully within ±5% of the observations. Our comparison meets the ASHRAE recommendations, so we extend VCWG's capability for the NV system study. Observation data for NV systems and building energy consumption for a group of buildings over a complete year is not currently accessible to the authors. However, in Section 3 we compare VCWG's predictions of cooling energy consumptions to other models published in the literature.

3. Results and discussion

We will begin this section with an analysis and discussion of the sensitivity study for the case of Toronto (CZ5) and Vancouver (CZ4). We will then provide an analysis of the prospects of NV systems in building cooling energy savings for the warmer climate zone of Phoenix (CZ3).

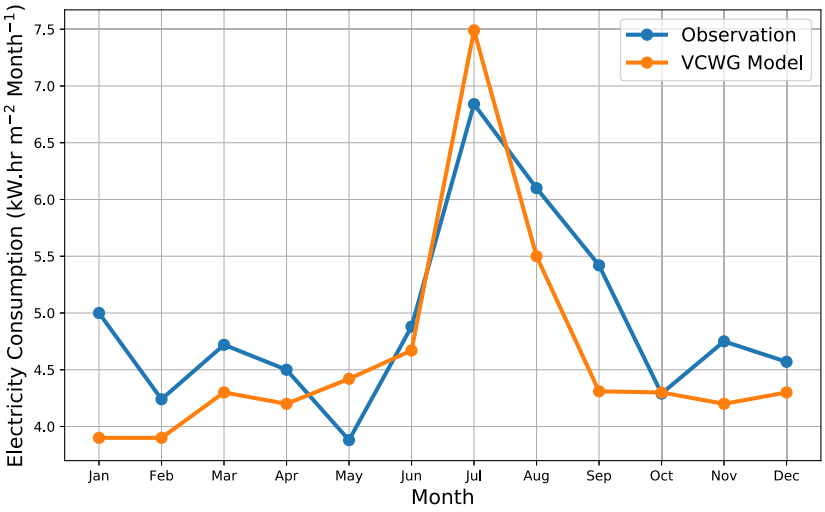

Fig. 6. Monthly electricity consumption in London, Ontario, as predicted by VCWG and measured in 2019.

3.1. Sensitivity analysis

Each simulation (detailed in Table 3) took approximately half an hour of computing time on a single CPU to complete for a full year analysis (2020). To analyze the thermal and energy behavior of the building for sensitivity analysis, seven key responses were simulated, as shown in Table 4, focusing on the impact of NV system on sensible cooling and latent loads. These responses include:

- R1: latent load (dehumidification/humidification, NV system assist); this response represents the latent load when NV system is assisting the HVAC system.
- R2: sensible cooling Load (NV system assist); this response represents the sensible cooling load when NV system is supplementing the HVAC system.
- R3: total cooling load (baseline case); this response represents the total cooling load of the base case scenario without NV system assistance. It includes both latent and sensible cooling loads.
- R4: total cooling load (NV system assist); this response is similar to R3, but incorporates the NV system assistance.
- R5: difference in total cooling load with NV system; this response quantifies the reduction in total cooling load achieved by enabling the NV system (R4 − R3).
- R6: difference in latent load with NV system; this response represents the change in latent load when the NV system is activated (difference between scenarios with and without NV system).
- R7: difference in sensible cooling load with NV system; this response represents the change in sensible cooling load when NV system is activated (difference between scenarios with and without NV system).

A third-order polynomial function was used to create fitting curves for the output results in relation to the independent variables: infiltration (ACH), R-value increase, and city. A second-order polynomial function was also considered, but it achieved a lower R-squared (R^2) value for the fit, so the third-order polynomial was preferred. Analysis of Variance (ANOVA) was then employed to evaluate how well these curves fit the simulated data. This analysis aimed to determine the statistical significance of the model's outputs in representing the findings. Table 4 presents the R-squared (R^2) values for all seven responses. As the table shows, all R-squared values exceed 90%, indicating a strong correlation between the modeled data and the simulated data. This result supports the reliability of the statistical assumptions made in the analysis. Furthermore, the F-value of the model is 33.44, which indicates statistical significance. There is only a 0.01% chance of observing an F-value of this magnitude by random chance. Additionally, the predicted R-squared and adjusted R-squared values for all responses are in close agreement, with a difference of less than 0.2. This agreement further strengthens the confidence in the model's ability to represent the findings.

Among all the cases in Table 2, two particular cases representing the base building features, Runs 4 for Vancouver and Run 11 for Toronto, will be examined now in greater detail to understand the model's behavior. In these cases, the building infiltration is set to 3 ACH and the total envelope thermal resistance is not increased.

The graph in Fig. 7 shows how the total sensible cooling demand changes month by month with and without NV. The graph shows that the sensible cooling demand is the highest in the summer and lowest in the shoulder seasons (spring and fall). In the winter, windows are mostly closed because there is almost no need for cooling. For Toronto, cooling demand is not present for January, October, November, and December. For Vancouver, it is not present for January, February, March, April, November, and December.

Table 3
Key responses for sensitivity analysis of Natural Ventilation (NV) impact on cooling loads. L: Latent Load, S: Sensible Load, T: Total Load (L+S), NV: Natural Ventilation [kW-hr m^{-2} $Year^{-1}$].

Run #	R1 L(NV)	R2 S(NV)	R3 T(Base)	R4 T(NV)	R5 T(Base)−T(NV)	R6 L(Base)−L(NV)	R7 S(Base)−S(NV)
1	36.7	65.0	107.4	101.7	5.7	−3.5	9.2
2	32.1	73.4	113.7	105.5	8.2	−2.1	10.2
19	34.7	66.1	107.8	100.7	7.1	−2.1	9.2
13	104.3	44.4	151.7	148.7	3.0	−1.5	4.5
6	100.1	47.6	149.0	147.6	1.4	−2.5	3.9
7	132.6	39.4	174.8	172.0	2.8	−0.6	3.4
16	137.5	38.7	177.9	176.1	1.8	−1.7	3.5
12	202.8	32.0	236.1	234.8	1.3	−0.3	1.7
4	230.7	29.7	262.1	260.3	1.8	−0.4	2.1
8	230.4	29.4	260.9	259.8	1.0	−0.6	1.7
20	230.3	29.4	261.5	259.8	1.8	−0.3	2.1
3	52.4	131.9	195.6	184.3	11.3	−2.4	13.7
10	46.1	123.4	186.6	169.6	17.0	−2.9	19.9
14	51.1	132.2	197.4	183.2	14.2	−2.1	16.2
18	138.2	103.4	252.3	241.6	10.7	−1.2	12.0
5	179.3	97.0	286.0	276.4	9.6	0.8	8.9
17	180.9	97.0	286.9	277.8	9.1	0.3	8.7
21	181.9	97.0	286.8	278.9	7.9	−0.5	8.5
9	272.9	73.5	353.7	346.4	7.3	0.8	6.6
11	308.9	84.4	397.8	393.4	4.5	0.3	4.1
15	308.6	83.1	396.3	391.7	4.7	−0.1	4.7

Table 4
R-Squared values for decision variables.

Output	R-Squared (R^2)
R1: Latent Load (NV)	99%
R2: Sensible Load (NV)	99%
R3: Total Load (Latent + Sensible) (Base)	99%
R4: Total Load (Latent + Sensible) (NV)	99%
R5: Total Load (Base − NV)	99%
R6: Latent Load (Base − NV)	88%
R7: Sensible Load (Base − NV)	98%

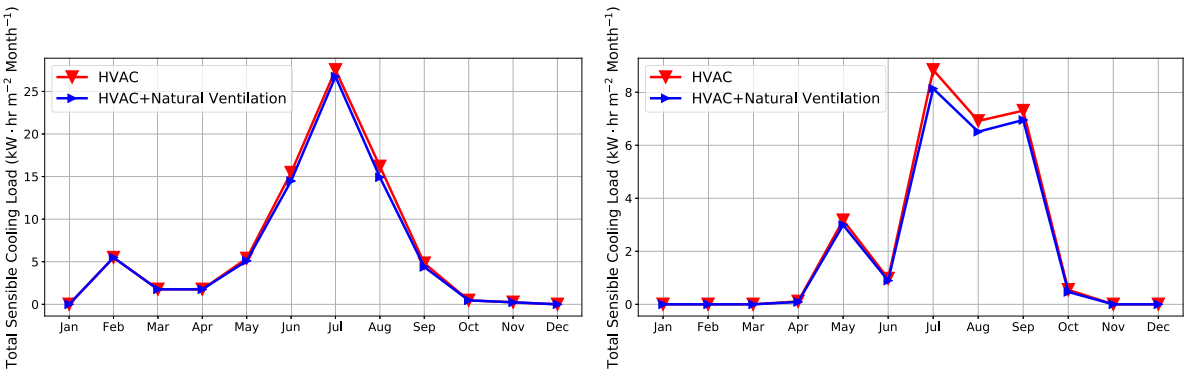

(a) Toronto (b) Vancouver

Fig. 7. Comparison of sensible cooling load under HVAC system-only mode versus HVAC system with Natural Ventilation (NV) assistance for (a) Toronto and (b) Vancouver, associated with building envelope thermal resistance increment of 0%, and infiltration of 3 ACH. (For interpretation of the references to color in this figure legend, the reader is referred to the web version of this article.)

The red line in the graph represents the cooling capacity provided solely by the HVAC system. The blue line depicts the scenario where the HVAC system is assisted by the NV system to achieve the desired cooling effect. The graph shows that Toronto has a much hotter summer than Vancouver. In Toronto, cooling loads can peak in July at around 27 kW-hr m^{-2} $Month^{-1}$, while in Vancouver it is only about 9 kW-hr m^{-2} $Month^{-1}$, which is just a third of Toronto's load. The biggest difference between the two lines (red and blue) happens in the hot months, from May to September for Toronto and Vancouver. This is when natural ventilation has the most potential to reduce the building sensible cooling demand.

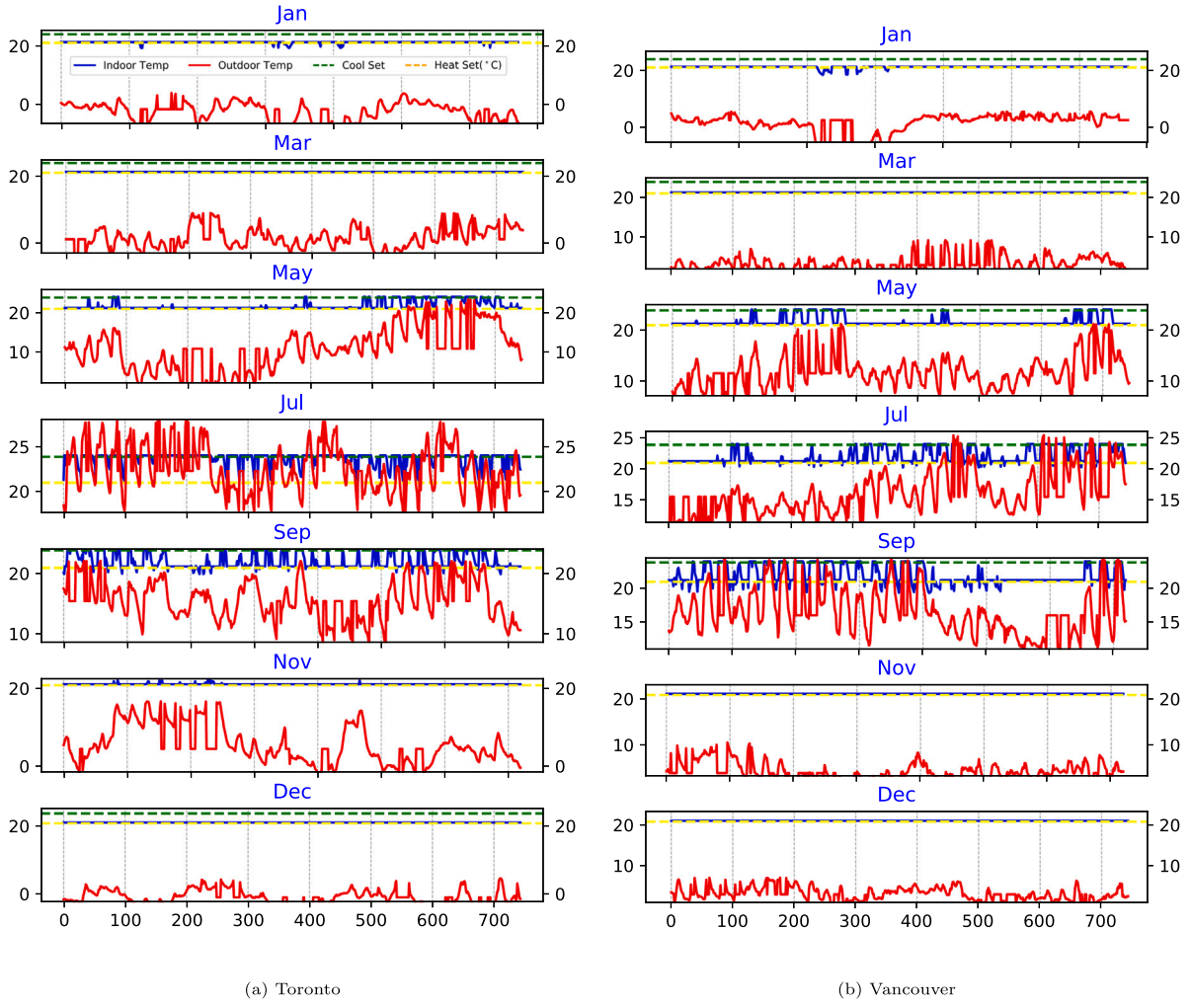

(a) Toronto (b) Vancouver

Fig. 8. Indoor and outdoor temperature [°C] variations across several chosen months in Toronto (left) and Vancouver (right), associated with typical building: envelope thermal resistance increment of 0% and infiltration of 3 ACH. (For interpretation of the references to color in this figure legend, the reader is referred to the web version of this article.)

Fig. 8 provides details on when windows are opened and under what temperature conditions for both Toronto and Vancouver. This figure shows how both indoor and outdoor temperatures change across seven chosen months. Each month is represented by two curves: a blue curve for indoor temperature and a red curve for outdoor temperature [°C]. The blue curve fluctuates between the cooling (green dotted line) and heating (yellow dotted line) temperature set-points. VCWG employs a two-step process to determine the indoor temperature and specific humidity. First, it calculates both the sensible and latent loads. Then, using separate diagnostic equations, it calculates the indoor temperature and specific humidity based on these loads. These calculated temperature and specific humidity values may potentially temporarily deviate from the established cooling and heating set-points, which can be seen in the figure. A closer look at this figure across different months reveals a pattern. During the shoulder and warm months, the outdoor temperature approaches the set-point temperatures. The state of the windows, open or closed, is heavily influenced by both indoor and outdoor temperatures. The specific conditions for window opening are outlined in Fig. 5. The indoor temperature needs to be higher than the set point temperature, and the outdoor temperature should be lower than the indoor temperature, for the NV system to be potentially triggered. Focusing on Toronto, a closer examination of January and March reveals that indoor temperatures primarily stay around the heating set-point (building under heating mode).

We next examine the model's performance in Toronto and Vancouver for the month of May in greater detail, as shown in Figs. 9 and 10, respectively. We will describe the physical behavior for the case of Toronto, although similar patterns are noticed for Vancouver. In May, the indoor temperature deviates from the heating set-point during certain periods due to cooling needs. We note two main periods when windows are predominantly open in Toronto: from 80 to 100 h and from 480 to 720 h (marked by gray dashed lines). Analyzing the temperature patterns during these periods helps us understand the functionality of the window opening algorithm. It becomes clear that windows have been opened when indoor temperatures are aligned with the cooling set-point

(green dotted) and outdoor temperature (red solid) is lower (colder) than the indoor temperature. Fig. 9 further demonstrates the well-maintained indoor environment within the building. Relative humidity levels primarily stay within the desired range of 40% (heating set-point, yellow dotted line) and 60% (cooling set-point, green dotted line). We examine a specific time period, consider 80–100 h. Here, we note that the conditions for window opening based on temperature are met (top). The middle plot then shows the indoor specific humidity is at the bottom of the acceptable range (corresponding to 40% relative humidity), indicating it remains below the cooling set point (corresponding to 60% relative humidity). This suggests that if the outdoor humidity is higher than indoor humidity at this time (red curve exceeding blue curve), it would create favorable conditions for NV. The figure confirms this, with outdoor specific humidity exceeding indoor specific humidity during these hours, allowing the algorithm to open the windows.

Towards the end of the month, as the windows are opened more frequently, the indoor specific humidity consequently increases. Interestingly, with the frequent window opening, the corresponding indoor relative humidity mostly stays around the 60% cooling set-point. This can be attributed to the gradual increase in indoor humidity caused by the introduction of more outdoor humid air through open windows, infiltration, and ventilation. As the indoor humidity approaches the cooling set-point, the model reduces the frequency of window opening to prevent further increase and by maintaining the specific humidity around the desired level. Since specific humidity cannot exceed the cooling set-point value, the model waits for outdoor specific humidity to decrease below the indoor specific humidity before window opening is considered again. This behavior can be observed between 600 and 650 h.

Due to the similarity of results between the Toronto and Vancouver cases, in the following figures, we only present the graphical results for Toronto. Fig. 11 illustrates the sensitivity of sensible cooling load (R2) to variations in building envelope thermal resistance (R-value) and infiltration rate (ACH) for the NV system in Toronto. Consistent with Fig. 7, Toronto exhibits notably higher sensible cooling loads (at least three times) compared to Vancouver (not shown). The plot reveals minimal sensitivity of sensible cooling load to R-value, with a slight decrease as R-value increases (reduced heat transfer). Conversely, the plot demonstrates a clear trend for infiltration: tighter building envelopes (lower ACH) lead to higher sensible cooling loads. This occurs because cooler outdoor air can effectively offset internal and solar heat gains when infiltration rates are high. It is important to note that internal and solar gains remain the primary contributors to the cooling load.

The analysis reveals that for cold climates like Canada, excessively airtight buildings may not be ideal for reducing sensible cooling loads, but air-tight buildings are required to reduce sensible heating demand [50]. Infiltration of cooler outdoor air can help reduce cooling needs for both Toronto and Vancouver. However, Toronto exhibits greater sensitivity to infiltration rate (ACH) due to its generally colder climate compared to Vancouver (not shown), except for July. Fig. 12 illustrates the difference in sensible cooling load with and without NV for Toronto. The plot demonstrates that the NV system can achieve notable savings in sensible cooling loads, reaching up to 20 kW-hr m^{-2} $Year^{-1}$. Notably, the savings increase modestly with higher R-values but show a dramatic rise with increased building air-tightness. For example, a typical building with a typical R-value and infiltration could only achieve savings of 5 kW-hr m^{-2} $Year^{-1}$ in Toronto.

Fig. 13 depicts the latent loads (R1) in Toronto for varying infiltration rates (ACH) and building envelope thermal resistances (R-value). Consistent with previous findings, Toronto exhibits higher loads than Vancouver (not shown) due to its more humid climate. A minimal change is noted with increasing R-value. However, Toronto shows slightly higher sensitivity, with a passive house (high R-value) experiencing lower latent loads (approximately a 6% reduction, or 20 kW-hr m^{-2} $Year^{-1}$). Conversely, the plot reveals a significant sensitivity to infiltration rate. Tighter buildings (lower ACH) have lower latent loads because less outdoor air, which is often outside the human comfort range in terms of humidity, enters the building.

When considering the difference in latent loads with and without the NV system (R6) (Fig. 14 for Toronto), the results suggest a potential drawback of the NV system. The plots show negative values throughout, indicating that using the NV system could lead to higher latent loads compared to the baseline scenario. This is due to the introduction of more outdoor air, which require additional latent load to maintain indoor comfort levels. This figure also exhibits a peak around a 50% increase in R-value, indicating an optimal level of building thermal resistance for maximizing latent load savings through NV.

Figs. 15 and 16 illustrate the total cooling loads for the case with and without the NV system, respectively, in Toronto. As noted previously, Toronto exhibits higher sensible cooling and latent loads in both cases than Vancouver (not shown). Toronto exhibits a greater sensitivity to changes in building envelope thermal resistance than Vancouver (not shown). Increasing the thermal resistance by 100% translates to a 12% reduction (15 kW-hr m^{-2} $Year^{-1}$) in the total cooling load. As discussed earlier, infiltration rate (ACH) has opposing effects on sensible and latent loads. Lower infiltration rate increases sensible cooling load as less outdoor air is introduced to remove heat. Conversely, it reduces latent loads by bringing in less outdoor moisture. However, the total cooling load diminishes with decreasing infiltration rate, as it is dominated by the latent load. In other words, this suggests that the reduction in latent loads outweighs the rise in sensible loads, making air-tightness a potential strategy for energy savings under cooling conditions. This highlights the dominance of latent loads in these climates.

Comparing the total cooling loads in the base case and the NV system, as presented in Fig. 17, demonstrates the clear benefits of NV. In Toronto and Vancouver (not shown), activating the NV system leads to a decrease in cooling load, ranging from 5 kW-hr m^{-2} $Year^{-1}$ for a typical building to 15 kW-hr kW-hr m^{-2} $Year^{-1}$ for an air-tight building. The results align with expectations by demonstrating greater total cooling load savings in Toronto compared to Vancouver. This can be attributed to Toronto's higher solar heat gain (leading to increased cooling demand) and its colder climate (providing a larger temperature difference for NV).

These findings align well with models and measurements from other studies in the field. For instance, a comprehensive experimental and numerical study by [63] conducted in London, UK, revealed an average annual cooling energy saving of 16.64 kW-hr m^{-2} $Year^{-1}$ through NV. Similarly, [64] reported a 24% reduction in cooling power consumption for Hong Kong using NV strategies, and [41] observed a 13% decrease in HVAC operation hours in Los Angeles.

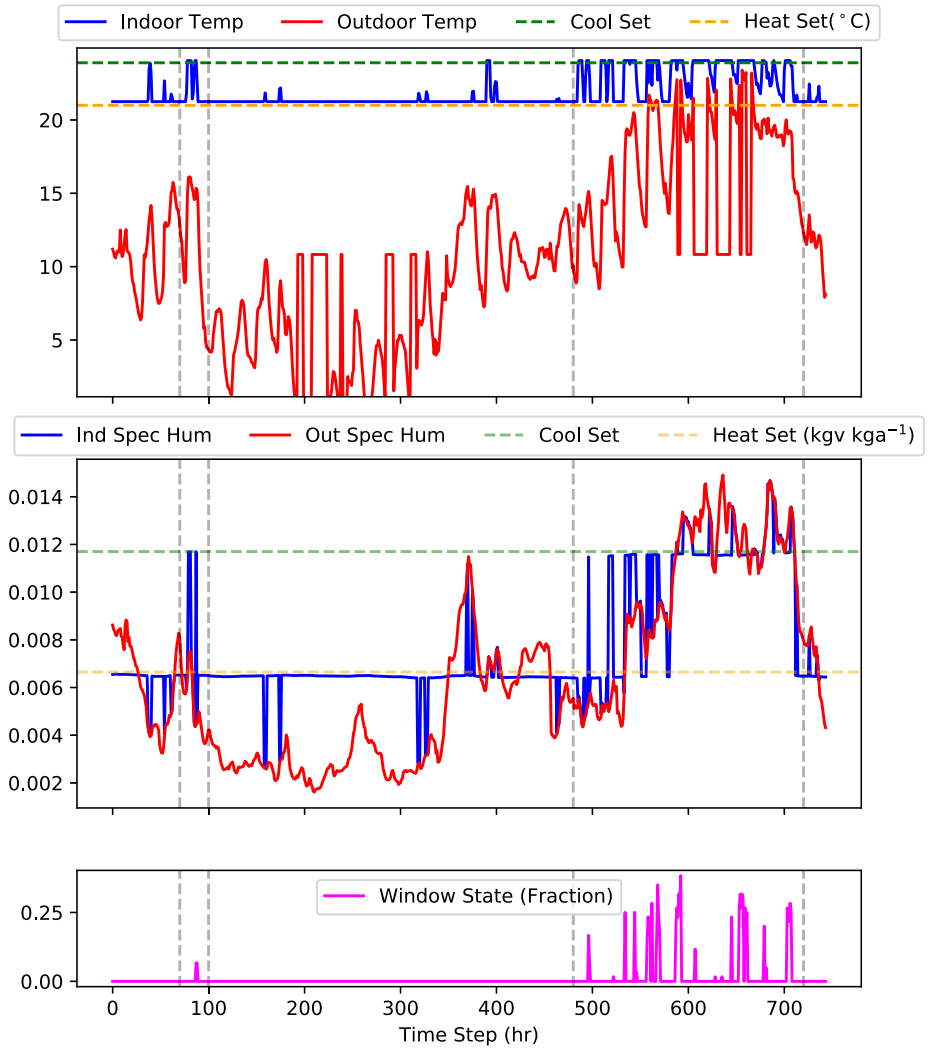

Fig. 9. Time series data for indoor and outdoor conditions in Toronto during May. Top panel: The variations in indoor (blue) and outdoor (red) temperatures [°C]. Middle panel: The indoor (blue) and outdoor (red) specific humidities [kgv kga^{-1}]. Bottom panel: The window state (fraction of the hour opened), associated with typical building: envelope thermal resistance increment of 0% and infiltration of 3 ACH. Main periods of window openings in Toronto are 80–100 h and 480–720 h, occurring when indoor temperatures align with the cooling set-point and outdoor temperatures are lower. (For interpretation of the references to color in this figure legend, the reader is referred to the web version of this article.)

3.2. Warmer climate zones

The amount of energy savings achieved through the NV system is heavily dependent on the outside weather conditions. To further investigate this, we conducted an additional simulation for Phoenix, Arizona, located in CZ3. As earlier simulations for Toronto and Vancouver showed (Fig. 7), for high infiltration rates (3 ACH), the cooling energy savings are small, so we chose a relatively air-tight building for the case of Phoenix with an infiltration of 0.3 ACH and no increase in R-value. Since Phoenix climate is more humid in the winter than in the summer (unlike Toronto and Vancouver), we used a relative humidity set point of 60% under the heating mode and 40% under the cooling mode. Through sensitivity analysis, it was found that such modification was necessary to achieve building energy savings using natural ventilation.

Fig. 18 shows the monthly sensible cooling consumption in Phoenix with and without NV. This figure reveals that, unlike Canadian cities where the NV system offers benefits primarily during the summer, Phoenix experiences the most notable benefits from the NV system during the winter months due to its hot climate. Additionally, our study suggests that NV primarily occurs at night when the outdoor temperature is low enough to provide effective cooling (not shown). The hourly variation of indoor/outdoor temperature, specific humidity and window state for Phoenix is shown in Fig. 19. Phoenix's climate enables night cooling, leading to a significantly higher frequency of window opening compared to Canadian cities. July was chosen for this analysis as it represents a month with fewer window opening opportunities, making it a clearer example. The figure illustrates that during specific hours

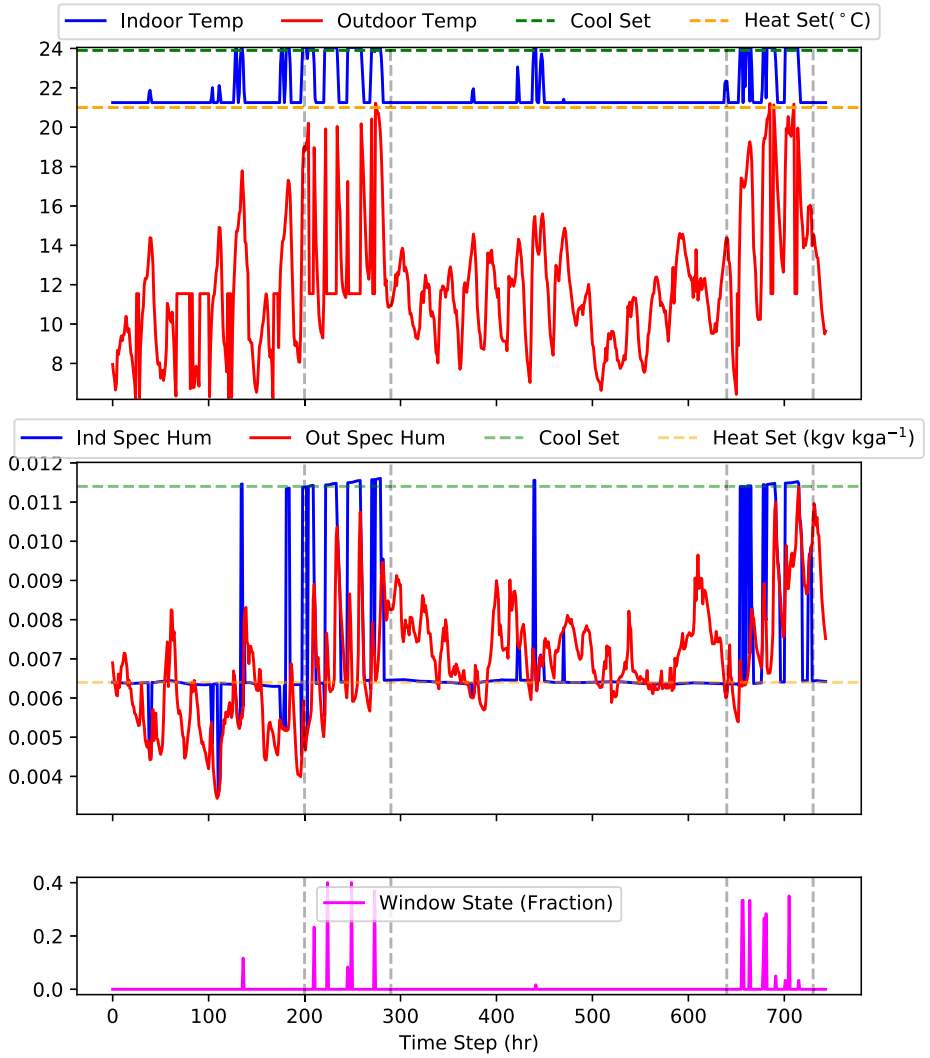

Fig. 10. Time series data for indoor and outdoor conditions in Vancouver during May. Top panel: The variations in indoor (blue) and outdoor (red) temperatures [°C]. Middle panel: The indoor (blue) and outdoor (red) specific humidities [kgv kga^{-1}]. Bottom panel: The window state (fraction of the hour opened), associated with typical building: envelope thermal resistance increment of 0% and infiltration of 3 ACH. Main periods of window openings in Vancouver are 200–290 h and 650–750 h, occurring when indoor temperatures align with the cooling set-point and outdoor temperatures are lower. (For interpretation of the references to color in this figure legend, the reader is referred to the web version of this article.)

(100–260, 380–450, and 690–730 h) the outdoor temperature falls below the cooling set-point, satisfying the first condition for night ventilation. However, the indoor humidity remains around 40% (set point under cooling mode), while the outdoor humidity is lower, creating extra latent load for window opening.

Comparing the results for the three cities in Fig. 20 and Table 5 (with infiltration rate 0.3 (ACH) and no increase in R-value) reveals that Phoenix, with its hotter climate (CZ3), has notably higher sensible cooling loads. However, using the NV system for sensible cooling load reduction is somewhat similar across all three cities, with Phoenix reaching a reduction of 8 kW-hr m^{-2} Year^{-1}. For latent cooling load, the energy needs are relatively close between the three cities. However, the NV system introduces some degree of moisture gain/loss, leading to increased latent loads for all three cities, with Phoenix exhibiting the greatest increase. In other words, the NV system helps saving sensible cooling loads, but it causes increases in latent loads. Overall, comparing the total savings potential, we note a trend where the opportunity for energy savings through the NV system decreases as we move towards lower climate zones (from CZ5 in Toronto to CZ3 in Phoenix); however, a more definitive statement, regarding such a trend, requires more extensive simulations across many more cities situated in different climate zones.

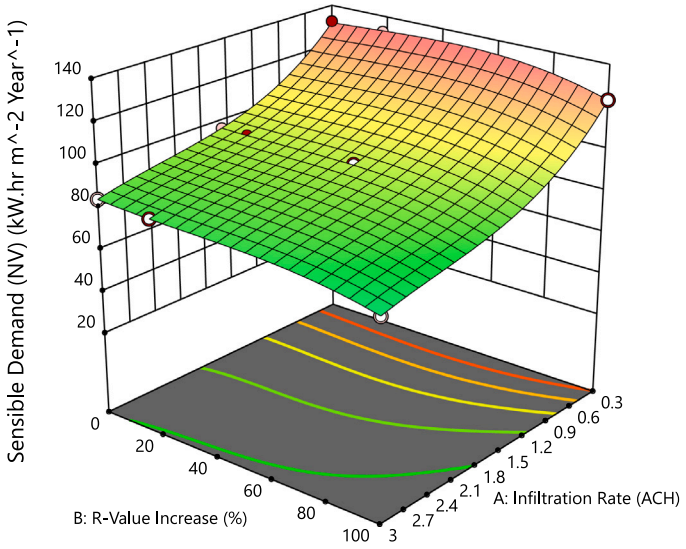

Fig. 11. Sensible cooling loads in Toronto.

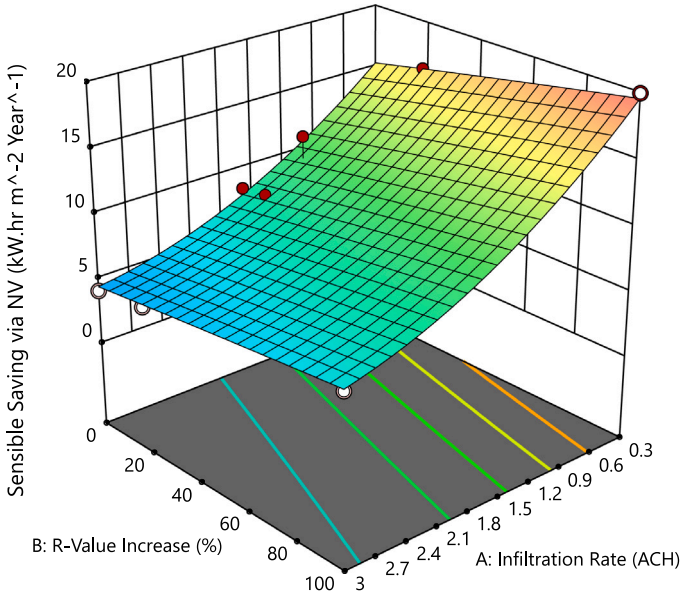

Fig. 12. Difference in sensible cooling load with and without NV system in Toronto.

Table 5
Differences [Savings(+)/Loss(−)] in sensible, latent, and total cooling loads [kW-hr m^{-2} $Year^{-1}$] as a result of using Natural Ventilation (NV) in Toronto, Vancouver, and Phoenix.

	Toronto (CZ5)	Vancouver (CZ4)	Phoenix (CZ3)
Sensible Cooling Load [Savings(+)/Loss(−)]	13	9	8
Latent Load [Savings(+)/Loss(−)]	2	−3	−6
Total Cooling Load [Savings(+)/Loss(−)]	15	6	2

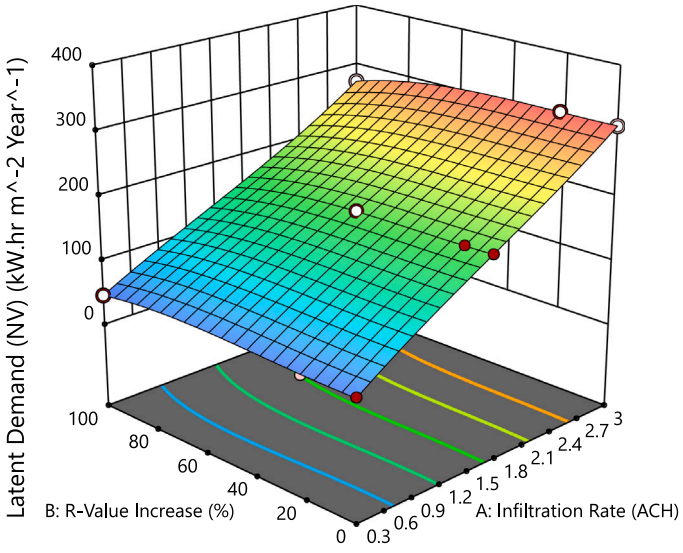

Fig. 13. Latent loads in Toronto.

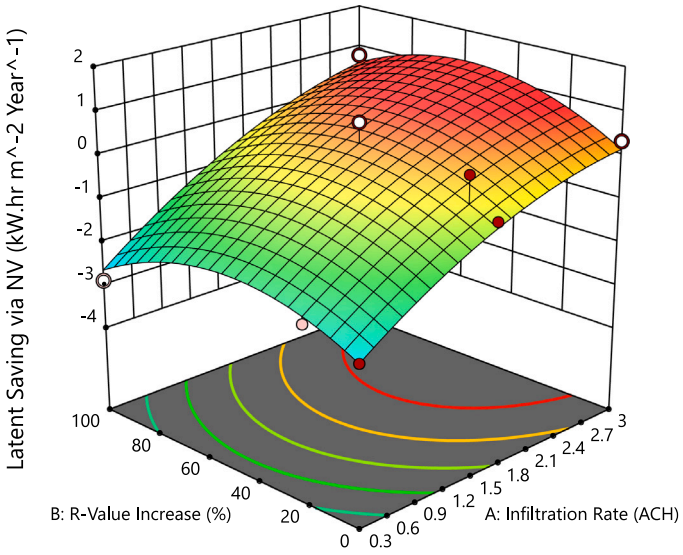

Fig. 14. Difference in latent loads with and without the NV system in Toronto.

3.3. Practical considerations

The above analysis shows that there are more aspects to be considered by building engineers when it comes to designing NV systems. Saving of building energy requires consideration of both sensible and latent loads while maintaining human thermal comfort. Designers should perform analysis of regional climatology for a building site, for which NV is considered. Long term hourly records of outdoor temperature and humidity are required, at least for a duration of one full year. Implementation of rules-based controls for NV requires monitoring of both indoor and outdoor temperature/humidity for operating doors and windows effectively. Set points for temperature and humidity control should be carefully designed considering long term analysis of climatology.

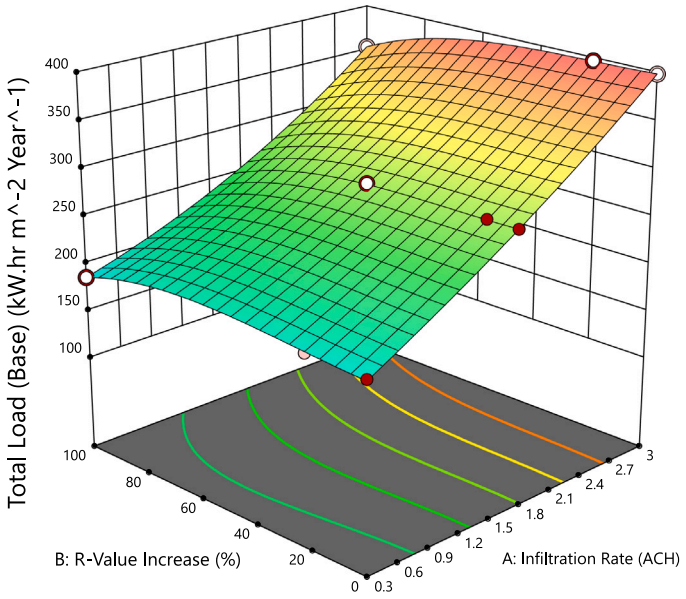

Fig. 15. Total cooling load (baseline) in Toronto.

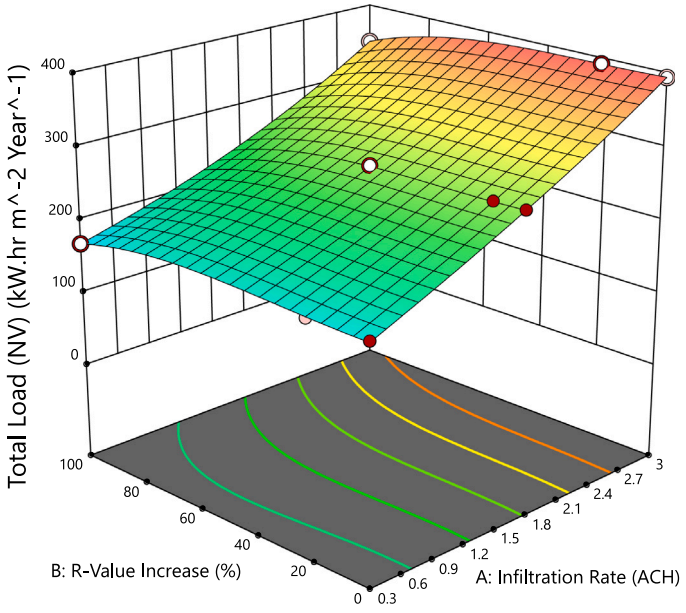

Fig. 16. Total cooling load (NV) in Toronto.

4. Conclusions and recommendations

In this paper, we developed and integrated a Natural Ventilation (NV) scheme into the Vertical City Weather Generator (VCWG v1.4.7) software. This allowed for a more comprehensive evaluation of building performance by accounting for the potential benefits of NV systems in saving sensible, latent, and total cooling energy demands, while simultaneously managing indoor temperature and humidity to maximize occupant comfort. Our model incorporated both sensible cooling and latent loads to achieve this, enabling us to optimize NV strategies for different Climate Zones (CZ). We studied three different cities by a full year simulation in 2020: Toronto (CZ5), Vancouver (CZ4), and Phoenix (CZ3). Our key findings highlight the potential role of NV systems in reducing energy consumption under cooling conditions:

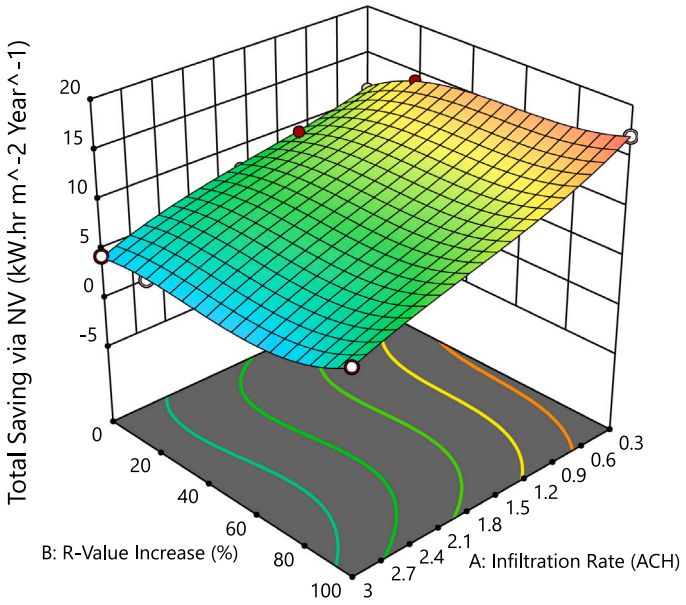

Fig. 17. Difference in total cooling load with and without Natural Ventilation (NV) in Toronto.

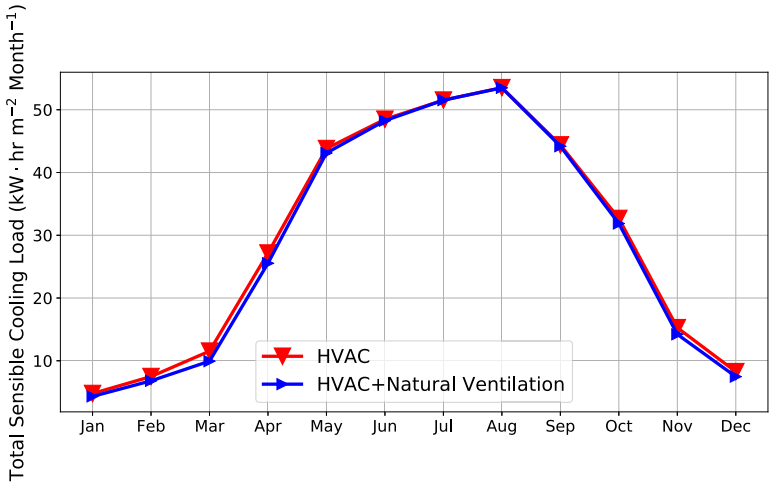

Fig. 18. Comparison of sensible cooling load under HVAC system-only mode versus HVAC system with Natural Ventilation (NV) assistance for Phoenix, associated with building envelope thermal resistance increment of 0% and infiltration of 0.3 ACH.

1. In cities with milder winters like Vancouver (CZ4), the NV system can be used for a longer period. Conversely, Toronto (CZ5) with colder winters sees shorter operational periods for the NV system. However, using NV, Toronto's hotter summers translate to a larger reduction in sensible cooling loads during peak months compared to Vancouver.
2. More air-tight buildings, while exhibiting lower latent loads, experience higher sensible cooling loads due to reduced NV.
3. Activation of NV systems in cities like Toronto and Vancouver, despite their vastly different summer cooling loads, leads to a decrease in total cooling load for both. These savings range from 5 kW-hr m^{-2} $Year^{-1}$ for typical buildings to 15 kW-hr m^{-2} $Year^{-1}$ for air-tight buildings, demonstrating that even typical buildings can benefit from NV strategies.
4. Toronto displayed a greater sensitivity to changes in building envelope thermal resistance compared to Vancouver. Doubling this resistance resulted in a substantial 12% reduction in Toronto's total cooling load.
5. NV offers decreasing energy savings potential as we move towards lower climate zones.
6. Adjusting the humidity set points under the cooling and heating modes for NV requires consideration of the climate context. Improper adjustment of humidity set points may result in the latent load of the building to increase beyond the savings of the sensible cooling load using NV, obscuring the benefits of NV.

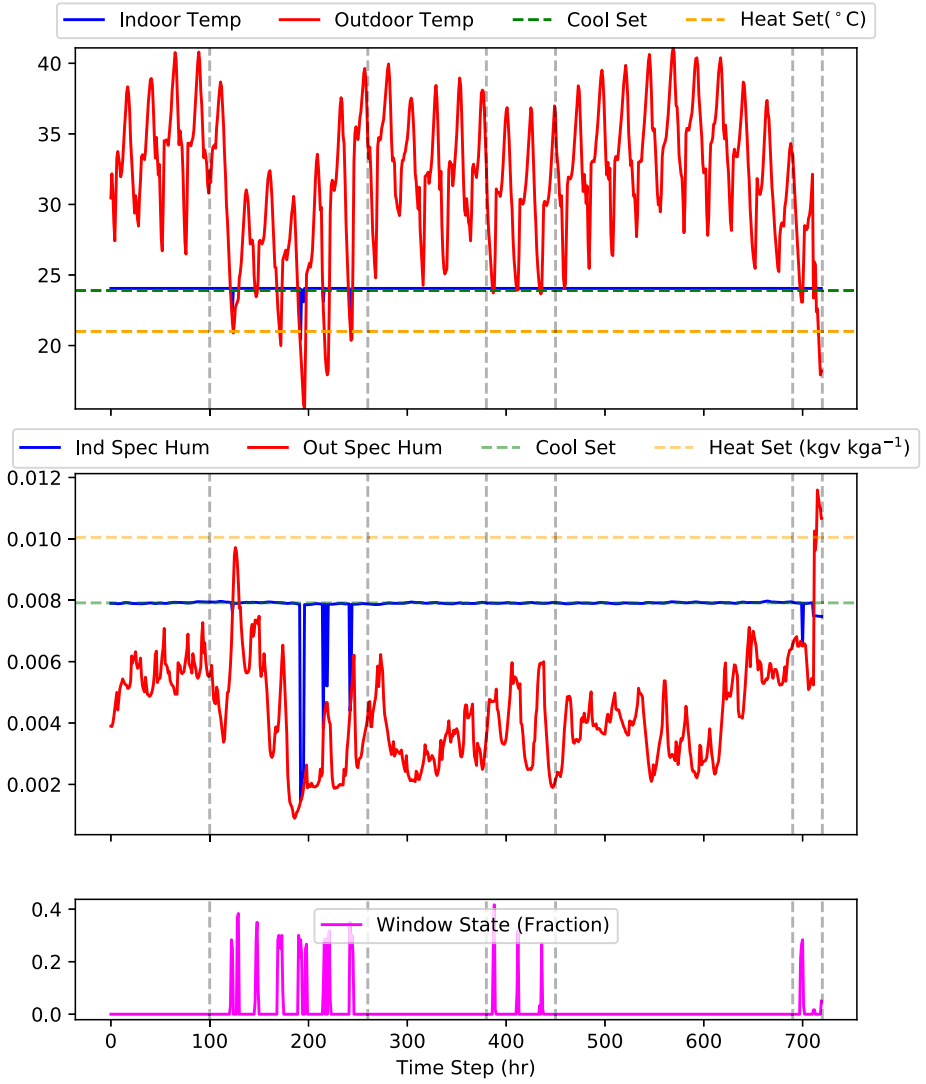

Fig. 19. Time series data for indoor and outdoor conditions in Phoenix during July. Top panel: The variations in indoor (blue) and outdoor (red) temperatures [°C]. Middle panel: The indoor (blue) and outdoor (red) specific humidities [kgv kga^{-1}]. Bottom panel: The window state (fraction of the hour opened), associated with typical building: envelope thermal resistance increment of 0% and infiltration of 0.3 ACH. Main periods of window openings in Phoenix are 100–260 h, 380–450 h, and 690–730 h, occurring when indoor temperatures align with the cooling set-point and outdoor temperatures are lower. (For interpretation of the references to color in this figure legend, the reader is referred to the web version of this article.)

Based on our findings, building and city designers should think about the compromises and conflicting nature of the sensible cooling versus latent loads. For example, if a building is designed to reduce the sensible cooling load using an NV system without attention to the complications in the latent load, it may confound the humidity comfort for the occupants.

Future work should investigate other mechanisms for natural ventilation beyond wind-driven ventilation, such as the buoyancy driven ventilation. Also advanced control schemes (e.g. fuzzy logic) may be considered for window operation, potentially leading to more energy-efficient NV strategies. Further, NV systems for other building types beyond the single detached residential houses may be investigated. Finally, detailed experimental observations may be carried out to confirm the findings of this study.

CRediT authorship contribution statement

Mojtaba Safdari: Writing – review & editing, Writing – original draft, Software, Methodology, Investigation, Data curation, Conceptualization. **Kadeem Dennis:** Writing – review & editing, Writing – original draft, Software, Methodology, Investigation, Formal analysis, Data curation. **Bahram Gharabaghi:** Writing – review & editing, Funding acquisition. **Kamran Siddiqui:** Writing – review & editing, Writing – original draft, Supervision, Funding acquisition. **Amir A. Aliabadi:** Writing – review & editing, Writing

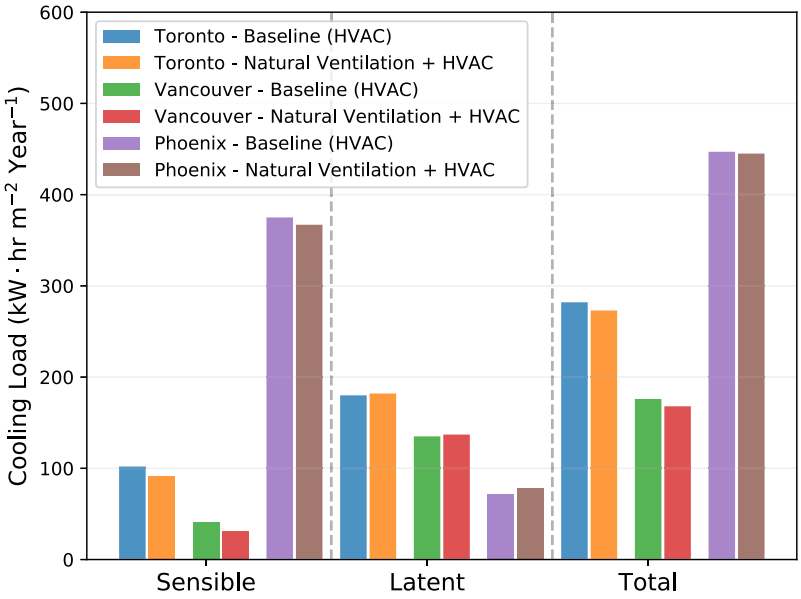

Fig. 20. Sensible, latent, and total cooling loads in Toronto, Vancouver, and Phoenix with and without Natural Ventilation (NV).

– original draft, Visualization, Validation, Supervision, Software, Methodology, Investigation, Funding acquisition, Formal analysis, Data curation.

Declaration of competing interest

The authors declare that they have no known competing financial interests or personal relationships that could have appeared to influence the work reported in this paper.

Data availability

The Atmospheric Innovations Research (AIR) Laboratory at the University of Guelph provides the model source code. For access, contact Amir A. Aliabadi (aaliabad@uoguelph.ca), visit http://www.aaa-scientists.com/, or visit https://github.com/AmirAAliabadi.

Acknowledgments

This work was supported by the University of Guelph through the International Doctoral Tuition Scholarship (IDTS); the Discovery Grant program (401231, 400675) from the Natural Sciences and Engineering Research Council (NSERC) of Canada; and the Climate Action and Awareness Fund (CAAF) (055725) from Environment and Climate Change Canada (ECCC).

Availability of code and data

The Atmospheric Innovations Research (AIR) Laboratory at the University of Guelph provides the model source code. For access, contact Amir A. Aliabadi (aaliabad@uoguelph.ca), visit http://www.aaa-scientists.com/, or visit https://github.com/AmirAAliabadi.

References

[1] R. Ruparathna, K. Hewage, R. Sadiq, Improving the energy efficiency of the existing building stock: A critical review of commercial and institutional buildings, Renew. Sustain. Energy Rev. 53 (2016) 1032–1045.
[2] S. Cao, C.W. Yu, X. Luo, New and emerging building ventilation technologies, Indoor Built Environ. 29 (4) (2020) 483–484.
[3] M. Safdari, R. Ahmadi, S. Sadeghzadeh, Numerical investigation on PCM encapsulation shape used in the passive-active battery thermal management, Energy 193 (2020) 116840.
[4] D.W. Etheridge, M. Sandberg, Building Ventilation: Theory and Measurement, vol. 50, John Wiley & Sons, Chichester, 1996.
[5] A.A. Aliabadi, S.N. Rogak, K.H. Bartlett, S.I. Green, Preventing airborne disease transmission: Review of methods for ventilation design in health care facilities, Adv Prev Med 2011 (2011) 124064, http://dx.doi.org/10.4061/2011/124064.
[6] M. Safdari, R. Ahmadi, S. Sadeghzadeh, Numerical and experimental investigation on electric vehicles battery thermal management under new European driving cycle, Appl. Energy 315 (2022) 119026.
[7] S. Yang, M.P. Wan, B.F. Ng, S. Dubey, G.P. Henze, W. Chen, K. Baskaran, Model predictive control for integrated control of air-conditioning and mechanical ventilation, lighting and shading systems, Appl. Energy 297 (2021).

[8] C. Wang, Y. Mei, H. Wang, X. Guo, T. Yang, C. Du, W. Yu, A predictive model for the growth diameter of mold under different temperatures and relative humidities in indoor environments, Buildings 14 (1) (2024).
[9] I. Petrova, V. Zaripova, Y. Lezhnina, I. Siddikov, Automated system for synthesis of sensors for smart cities, E3S Web Conf. 97 (2019) 01023, http://dx.doi.org/10.1051/e3sconf/20199701023.
[10] W. Li, Optimal Control of Air-Conditioning Systems for Enhanced Indoor Environment and Energy Efficiency Using IoT-based Smart Sensors (Ph.D. thesis), Hong Kong Polytechnic University, Hong Kong, 2021.
[11] E.E. Broday, M.C. Gameiro da Silva, The role of Internet of Things (IoT) in the assessment and communication of indoor environmental quality (IEQ) in buildings: a review, Smart Sustain. Built Environ. 12 (3) (2023).
[12] A. Zivelonghi, A. Giuseppi, Smart healthy schools: An IoT-enabled concept for multi-room dynamic air quality control, Internet Things Cyber-Phys. Syst. 4 (2024) 24–31.
[13] A. Karpenko, I. Petrova, Control indoor climate, in: 2017 8th International Conference on Information, Intelligence, Systems and Applications, IISA, 2017, pp. 1–6, http://dx.doi.org/10.1109/IISA.2017.8316432.
[14] F. Liu, A. Chang-Richards, I. Kevin, K. Wang, K.N. Dirks, Effects of indoor environment factors on productivity of university workplaces: A structural equation model, Build. Environ. 233 (2023).
[15] Y. Zhao, D. Li, Multi-domain indoor environmental quality in buildings: A review of their interaction and combined effects on occupant satisfaction, Build. Environ. 228 (2023).
[16] P. Wargocki, J.A. Porras-Salazar, S. Contreras-Espinoza, W. Bahnfleth, The relationships between classroom air quality and children's performance in school, Build. Environ. 173 (2020) 106749.
[17] M.J. Alonso, P. Liu, S.F. Marman, R.B. Jørgensen, H.M. Mathisen, Holistic methodology to reduce energy use and improve indoor air quality for demand-controlled ventilation, Energy Build. 279 (2023).
[18] S. Li, Review of engineering controls for indoor air quality: A systems design perspective, Sustainability 15 (19) (2023).
[19] K. Abhijith, V. Kukadia, P. Kumar, Investigation of air pollution mitigation measures, ventilation, and indoor air quality at three schools in London, Atmos. Environ. 289 (2022).
[20] F. Ibrahim, E.Z. Samsudin, A.R. Ishak, J. Sathasivam, Hospital indoor air quality and its relationships with building design, building operation, and occupant-related factors: A mini-review, Front. Public Health 10 (2022) 1067764.
[21] S. Nguyen, et al., Thermal Comfort in Indoor Sports Facilities and the Adequacy of Demand-controlled Ventilation (Master's thesis), Aalto University, Espoo, 2023.
[22] A. O'Donovan, M.D. Murphy, P.D. O'Sullivan, Passive control strategies for cooling a non-residential nearly zero energy office: Simulated comfort resilience now and in the future, Energy Build. 231 (2021) 110607.
[23] E.T. Maddalena, Y. Lian, C.N. Jones, Data-driven methods for building control—A review and promising future directions, Control Eng. Pract. 95 (2020).
[24] C. Ren, S.-J. Cao, Implementation and visualization of artificial intelligent ventilation control system using fast prediction models and limited monitoring data, Sustainable Cities Soc. 52 (2020) 101860.
[25] J. Cheng, D. Qi, A. Katal, L.L. Wang, T. Stathopoulos, Evaluating wind-driven natural ventilation potential for early building design, J. Wind Eng. Ind. Aerodyn. 182 (2018) 160–169.
[26] X. Meng, Y. Wang, X. Xing, Y. Xu, Experimental study on the performance of hybrid buoyancy-driven natural ventilation with a mechanical exhaust system in an industrial building, Energy Build. 208 (2020) 109674.
[27] J.M. Rey-Hernández, J.F. San José-Alonso, E. Velasco-Gómez, C. Yousif, F.J. Rey-Martínez, Performance analysis of a hybrid ventilation system in a near zero energy building, Build. Environ. 185 (2020) 107265.
[28] X. Cheng, Z. Shi, K. Nguyen, L. Zhang, Y. Zhou, G. Zhang, J. Wang, L. Shi, Solar chimney in tunnel considering energy-saving and fire safety, Energy 210 (2020) 118601.
[29] C. Walker, L. Glicksman, Reduced-scale air modeling technique for naturally ventilated buildings, in: Research in Building Physics and Building Engineering, CRC Press, 2020, pp. 713–719.
[30] M.W. Liddament, M. Orme, Energy and ventilation, Appl. Therm. Eng. 18 (1998) 1101–1109, http://dx.doi.org/10.1016/s1359-4311(98)00040-4.
[31] P.W. Tien, S. Wei, T. Liu, J. Calautit, J. Darkwa, C. Wood, A deep learning approach towards the detection and recognition of opening of windows for effective management of building ventilation heat losses and reducing space heating demand, Renew. Energy 177 (2021) 603–625.
[32] C. Allocca, Q. Chen, L.R. Glicksman, Design analysis of single-sided natural ventilation, Energy Build. 35 (8) (2003) http://dx.doi.org/10.1016/S0378-7788(02)00239-6.
[33] G. Tan, L.R. Glicksman, Application of integrating multi-zone model with CFD simulation to natural ventilation prediction, Energy Build. 37 (10) (2005) http://dx.doi.org/10.1016/j.enbuild.2004.12.009.
[34] Y. Peng, Y. Lei, Z.D. Tekler, N. Antanuri, S.-K. Lau, A. Chong, Hybrid system controls of natural ventilation and HVAC in mixed-mode buildings: A comprehensive review, Energy Build. 276 (2022).
[35] M. Rabani, V. Kalantar, A.A. Dehghan, A.K. Faghih, Empirical investigation of the cooling performance of a new designed trombe wall in combination with solar chimney and water spraying system, Energy Build. 102 (2015) 45–57, http://dx.doi.org/10.1016/j.enbuild.2015.05.010.
[36] Y. Wu, N. Gao, J. Niu, J. Zang, Q. Cao, Numerical study on natural ventilation of the wind tower: Effects of combining with different window configurations in a low-rise house, Build. Environ. 188 (2021) 107450.
[37] J.K. Calautit, D. O'Connor, P.W. Tien, S. Wei, C.A.J. Pantua, B. Hughes, Development of a natural ventilation windcatcher with passive heat recovery wheel for mild-cold climates: CFD and experimental analysis, Renew. Energy 160 (2020) 465–482.
[38] S.-Y. Wu, L.-F. Wu, L. Xiao, Effects of aspect ratio and inlet wind velocity on thermal characteristics of Trombe wall channel under different ventilation strategies: An indoor experiment, Exp. Therm Fluid Sci. 141 (2023).
[39] M. Luo, Y. Hong, J. Pantelic, Determining building natural ventilation potential via IoT-based air quality sensors, Front. Environ. Sci. 9 (2021) 634570.
[40] Y. Zhai, A. Honnekeri, M. Pigman, M. Fountain, H. Zhang, X. Zhou, E. Arens, Use of adaptive control and its effects on human comfort in a naturally ventilated office in Alameda, California, Energy Build. 203 (2019) 109435.
[41] Y. Chen, L.K. Norford, H.W. Samuelson, A. Malkawi, Optimal control of HVAC and window systems for natural ventilation through reinforcement learning, Energy Build. 169 (2018) 195–205.
[42] V.J. Gan, M. Deng, Y. Tan, W. Chen, J.C. Cheng, BIM-based framework to analyze the effect of natural ventilation on thermal comfort and energy performance in buildings, Energy Procedia 158 (2019) 3319–3324.
[43] H. Zhang, D. Yang, V.W. Tam, Y. Tao, G. Zhang, S. Setunge, L. Shi, A critical review of combined natural ventilation techniques in sustainable buildings, Renew. Sustain. Energy Rev. 141 (2021) 110795.
[44] M. Eftekhari, L. Marjanovic, Application of fuzzy control in naturally ventilated buildings for summer conditions, Energy Build. 35 (7) (2003) 645–655.
[45] A. Aliabadi, Turbulence: A Fundamental Approach for Scientists and Engineers, Springer, Cham, 2022, http://dx.doi.org/10.1007/978-3-030-95411-6.
[46] A.A. Aliabadi, M. Moradi, R.M. McLeod, D. Calder, R. Dernovsek, How much building renewable energy is enough? The vertical city weather generator (VCWG v1.4.4), Atmosphere 12 (7) (2021) 882, http://dx.doi.org/10.3390/atmos12070882.
[47] M. Moradi, B. Dyer, A. Nazem, M.K. Nambiar, M.R. Nahian, B. Bueno, C. Mackey, S. Vasanthakumar, N. Nazarian, E.S. Krayenhoff, L.K. Norford, A.A. Aliabadi, The Vertical City Weather Generator (VCWG v1.3.2), Geosci. Model Dev. 14 (2) (2021) 961–984, http://dx.doi.org/10.5194/gmd-14-961-2021.
[48] M. Moradi, The Vertical City Weather Generator (Ph.D. thesis), University of Guelph, Guelph, 2021.

[49] M. Moradi, E.S. Krayenhoff, A.A. Aliabadi, A comprehensive indoor–outdoor urban climate model with hydrology: The Vertical City Weather Generator (VCWG v2.0.0), Build. Environ. 207 (2022) 108406, http://dx.doi.org/10.1016/j.buildenv.2021.108406.
[50] A.A. Aliabadi, X. Chen, J. Yang, A. Madadizadeh, K. Siddiqui, Retrofit optimization of building systems for future climates using an urban physics model, Build. Environ. 243 (2023) 110655, http://dx.doi.org/10.1016/j.buildenv.2023.110655.
[51] A.A. Aliabadi, R.M. McLeod, The Vatic Weather File Generator (VWFG v1.0.0), J. Build. Eng. 67 (2023) 105966, http://dx.doi.org/10.1016/j.jobe.2023.105966.
[52] NRCan, National Energy Use Database, Technical Report, Office of Energy Efficiency, Natural Resources Canada, Gatineau, 2020.
[53] US Census Bureau, American Community Survey (ACS), Technical Report, United States Census Bureau, Washington, 2020.
[54] NRCan, National Energy Code of Canada, Technical Report, Office of Energy Efficiency, Natural Resources Canada, Gatineau, QC, 2017.
[55] ASHRAE, Standard 62.1: Ventilation and Acceptable Indoor Air Quality, Technical Report, American Society for Heating Refrigeration and Airconditioning Engineers, Peachtree Corners, 2022.
[56] ASHRAE, Standard 62.2: Ventilation and Acceptable Indoor Air Quality in Residential Buildings, Technical Report, American Society for Heating Refrigeration and Airconditioning Engineers, Peachtree Corners, 2022.
[57] ASHRAE, Standard 90.1: Energy Standard for Buildings Except Low-Rise Residential Buildings, Technical Report, American Society for Heating Refrigeration and Airconditioning Engineers, Peachtree Corners, 2013.
[58] ASHRAE, Standard 90.2: Energy-Efficient Design of Low-Rise Residential Buildings, Technical Report, American Society for Heating Refrigeration and Airconditioning Engineers, Peachtree Corners, 2018.
[59] ASHRAE, ASHRAE Handbook - Fundamentals, Technical Report, American Society for Heating Refrigeration and Airconditioning Engineers, Peachtree Corners, 2021.
[60] Passive-House-Institute, Criteria for the Passive House EnerPHit and PHI Low Energy Building Standard, Technical Report, Passive House Institute, Darmstadt, 2015.
[61] ASHRAE, Standard 140: Standard Method Of Test For The Evaluation Of Building Energy Analysis Computer Programs, Technical Report, American Society for Heating Refrigeration and Airconditioning Engineers, Peachtree Corners, 2017.
[62] ASHRAE, Guideline 14: Measurement of Energy, Demand, and Water Savings, Technical Report, American Society for Heating Refrigeration and Airconditioning Engineers, Peachtree Corners, 2014.
[63] J. Song, X. Huang, D. Shi, W.E. Lin, S. Fan, P.F. Linden, Natural ventilation in London: Towards energy-efficient and healthy buildings, Build. Environ. 195 (2021) 107722.
[64] F.W. Yik, Y.F. Lun, Energy saving by utilizing natural ventilation in public housing in Hong Kong, Indoor Built Environ. 19 (1) (2010) 73–87.